AIP | Applied Physics Letters

Experimental verification of total absorption by a low-loss thin dielectric layer

Ana Díaz-Rubio, Alastair P. Hibbins, Jorge Carbonell, and José Sánchez-Dehesa

Citation: Applied Physics Letters **106**, 241604 (2015); doi: 10.1063/1.4922801
View online: http://dx.doi.org/10.1063/1.4922801
View Table of Contents: http://scitation.aip.org/content/aip/journal/apl/106/24?ver=pdfcov
Published by the AIP Publishing

Experimental verification of total absorption by a low-loss thin dielectric layer

Ana Díaz-Rubio,[1,a)] Alastair P. Hibbins,[2] Jorge Carbonell,[1] and José Sánchez-Dehesa[1,a)]
[1]*Wave Phenomena Group, Department of Electronic Engineering, Universitat Politècnica de València, Camino de Vera S/N. (Building 7F1), ES-46022 Valencia, Spain*
[2]*Electromagnetic and Acoustic Materials Group, Department of Physics and Astronomy, University of Exeter, Stocker Road, Exeter EX4 4QL, United Kingdom*

(Received 29 January 2015; accepted 6 June 2015; published online 19 June 2015)

This work presents an experimental demonstration of total absorption by a metal-dielectric metasurface. Following a theoretical proposal [Díaz-Rubio *et al.*, Phys. Rev. B **89**, 245123 (2014)], we have designed and fabricated a metasurface consisting of a low absorbing dielectric layer (made of FR4) placed on top of a metallic surface patterned with a square array of coaxial cavities. For p-polarized waves, a low frequency peak with perfect absorption is observed. The behavior of this peak has been experimentally characterized for different dielectric layer thicknesses, coaxial cavity lengths, and angles of incidence. The experimental results are in excellent agreement with numerical simulation and corroborate the theoretical predictions. © *2015 AIP Publishing LLC*.
[http://dx.doi.org/10.1063/1.4922801]

Electromagnetic absorbers have attracted much interest due to the number of applications in which they are involved. However, the design of flat and thin materials with high absorption is still a challenge. Recently, the introduction of metamaterials has opened ways for designing absorbing materials. Metamaterials are artificial structures whose elements are arranged periodically on a subwavelength scale and they exhibit unusual properties not found in natural materials.[1,2] Working under the homogenization limit, the periodic system can be considered as an effective medium whose behavior can be tailored almost without limitations. These artificial materials have been proposed for many interesting applications like perfect lenses, optical cloaking, and perfect absorbers.[3–5] If the metamaterial approach to the design of high-performance absorbers is to yield success, then any prototype device will be required to satisfy at least one of the following criteria: (i) perfect or near unity absorption, (ii) very thin or sub-wavelength size to avoid bulky devices, and (iii) broadband operation. To these purposes, a number of options have been already proposed. For example, structures based on resonant patches[6,7] have been studied at several spectral regimes. Usually, the resonant characteristics of these patches are employed to optimize absorption. Also, in combination with metallic backed planes, thin layers have been studied including slits in dielectric layers,[8,9] holes or cavities in the metallic plane,[10,11] and even metal-dielectric multilayered structures.[12] Wide incidence angles can be explored with any of these possible element configurations.[13] Also, if the sub-wavelength thickness requirement is relaxed, performance improvements in broadband operation can be achieved.[14,15]

Previously, some of the current authors proposed a strongly absorbing "metasurface" for microwave frequencies consisting of a thin layer made of a low loss dielectric material on top of a patterned metallic plate,[16] and they emphasized its ability to tune the frequency of the absorption peak. The metallic plate under consideration consisted of a square array of closely spaced (non-diffracting) air-filled coaxial cavities. For p- (transverse magnetic, TM) polarized waves, it was proven that the strong localization of electromagnetic energy in the coaxial cavities at the resonant frequencies enhances the energy absorption in the dielectric slab on top, yielding peaks of total absorption. These absorption peaks appeared at wavelengths one order of magnitude larger than the thickness of the dielectric slab. Moreover, it was also demonstrated that the frequency position of the absorption peak mainly depends on the cavity length; the other physical parameters of the design only change slightly its position.

In this Letter, we experimentally study the absorbing system introduced in Ref. 16 and present a practical demonstration of the easy tunable system theoretically proposed. In particular, a metasurface producing total absorption is designed, fabricated, and experimentally characterized, studying the influence of the angle of incidence. The control of the peak frequency with the cavity length is demonstrated, and the dependence of the peak amplitude with the dielectric thickness is also shown. Figure 1(a) provides a schematic representation of the proposed structures showing the main parameters involved for their manufacturing. A photograph of one constructed metasurface is shown in Figure 1(b), where the dielectric layer is slightly displaced from its original position for a better visualization of the square array of circular coaxial cavities. The dielectric material chosen for the experimental demonstration is a glass-reinforced epoxy laminate of FR4 type. At the operation frequencies, the dielectric permittivity of this material is $\varepsilon_d = 4.2(1 + 0.025i)$.[17] Let us point out that the small imaginary part of this permittivity indicates that FR4 has a poor performance as an absorber of microwaves frequencies. Particularly, we have designed a metasurface made of aluminum which can enhance the absorption of

a)Authors to whom correspondence should be addressed. Electronic addresses: andiaru@hma.upv.es and jsdehesa@upv.es.

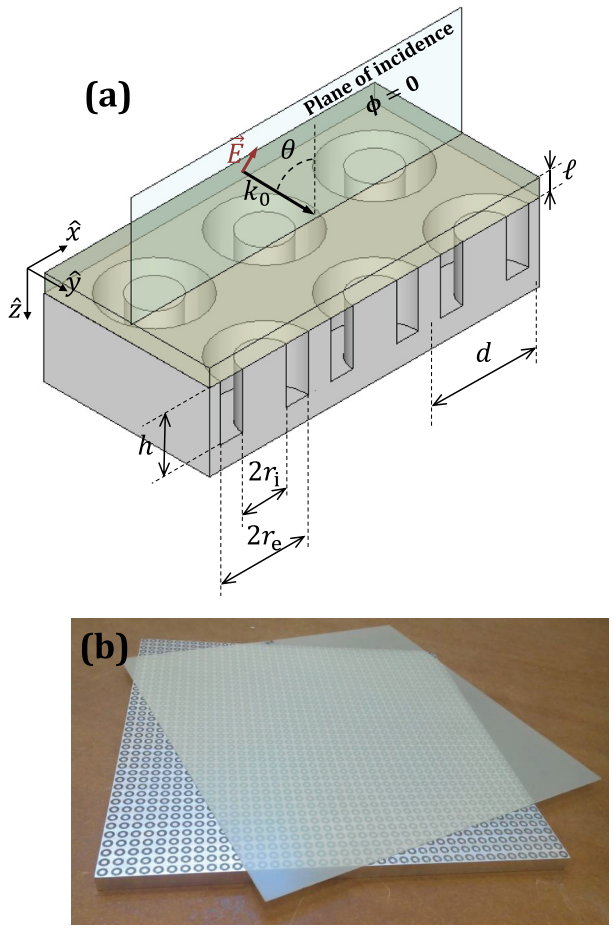

FIG. 1. (a) Schematic representation of the fabricated devices consisting of an array of coaxial cavities in a metal covered by a dielectric sheet. The plane of incidence is also shown. (b) Photograph of one constructed device. The FR4 dielectric layer is displaced for a better observation of the patterned surface, which has parameters: $d = 10\,\text{mm}$, $r_i = 2\,\text{mm}$, and $r_e = 4\,\text{mm}$.

a FR4 layer with $\ell = 1.2\,\text{mm}$, producing total absorption. After choosing the FR4 dielectric layer, we have designed the coaxial-cavity grating for having a total absorption peak in the frequency range between 5 GHz and 10 GHz, which is below the diffraction limit. To ensure that, we define the lattice constant $d = 10\,\text{mm}$. Then, the physical dimensions of the cavity cross section, taking into account the fabrication limitation, are: $r_e = 4\,\text{mm}$ and $r_i = 2\,\text{mm}$ the external and internal radius, respectively. Selection of the peak frequency, f, and the cavity length, h, is done using the expressions extracted from the low-frequency and monomode approximation in Ref. 16. See Sec. 2 in the supplementary material[18] for a detailed description of the design expressions extracted from the simplified model and their application for the design of total absorption devices. On the one hand, we can determine the cavity length and extract the frequency from the design expressions. For example, defining the cavity length $h = 10\,\text{mm}$, we know that the absorption peak appears at $f = 5.62\,\text{GHz}$. On the other hand, we can set the frequency and find the cavity length which ensures the absorption peak at this frequency. In this case, the goal is to obtain a total absorption peak at $f = 7.1\,\text{GHz}$ and from the theoretical expressions we obtain that the needed cavity length is $h = 7\,\text{mm}$.

For the verification of our designs and the study of the effects produced by the cavity length and the dielectric thickness, we have studied the combination of three cavity lengths and three dielectric thicknesses. The three different cavity lengths are $h = 10\,\text{mm}$ (sample 1), 7 mm (sample 2), and 5 mm (sample 3). The samples consist of 40 unit cells in the x-direction and 40 unit cells in the y-direction, and the periodicity of the array is $d = 10\,\text{mm}$. The dielectric sheet entirely covers the metallic grating and it is fixed at the corners. Also we have characterized the coaxial-cavity grating with three different dielectric thicknesses, $\ell = 1.2\,\text{mm}$ (slab 1), 1.6 mm (slab 2), and 2.3 mm (slab 3). Thus, a total number of nine different structures have been experimentally characterized in this work.

In the experimental setup, a microwave front radiated from a rectangular horn antenna, which is placed at the focus of a collimating spherical mirror, impinges with an incident angle θ on the fabricated sample. The horn antenna is orientated and positioned such that the electric-vector of the radiation is in the plane of incidence (i.e., p- or TM polarized), and so that the plane is incidence is parallel to the xz-plane [keeping $\phi = 0$, see Fig. 1(a)]. The reflected beam is collected by a receiver horn antenna, which is orientated to detect only p-polarized radiation and placed at the focus of a second mirror tilted an angle θ with respect to the normal vector of the sample surface. The angle of incidence is shifted manually by changing the position and rotation of the transmission and the detection horns. A reference measurement is needed for obtaining the absorption spectra. This reference measurement is taken by replacing the device with an aluminum plate that has the same surface area and thickness as that of the sample (with the dielectric layer). The reflectivity is obtained for the same frequency (f) values with the sample and with the reference plate. Using this method, the sample absorption (A) can be calculated from

$$A(f) = 1 - \frac{R_{\text{device}}(f)}{R_{\text{ref}}(f)}, \tag{1}$$

where $R_{\text{device}}(f)$ and $R_{\text{ref}}(f)$ are the reflectivity spectra for the sample and the aluminum plate, respectively.

Figure 2 summarizes the experimental characterization of sample 1 ($h = 10\,\text{mm}$) with slab 1 ($\ell = 1.2\,\text{mm}$) on top. In Figure 2(a), the absorption spectrum is shown when the incident angle is $\theta = 45°$. The symbols represent the experimental data, while the continuous line is the calculated with the model based on the mode matching technique reported in Ref. 16. For the comprehensiveness of this work, an account of the model can be found in Sec. 1 of the supplementary material.[18] The dashed line corresponds to the absorption produced with the dielectric layer (slab 1) covering an unpatterned aluminum surface. It is observed that the calculated spectrum is in good agreement with the experimental one except for a small frequency shift: the measured peak centered at 5.62 GHz gives absorption of 93% while the calculated peak is centered at 5.5 GHz with 98% absorption. The shifting of the measured peak towards high frequencies is about 2% and is due to an unavoidable air film existing between the metal grating and the dielectric layer. This film of air or air gap appears because of the defects (raised edges)

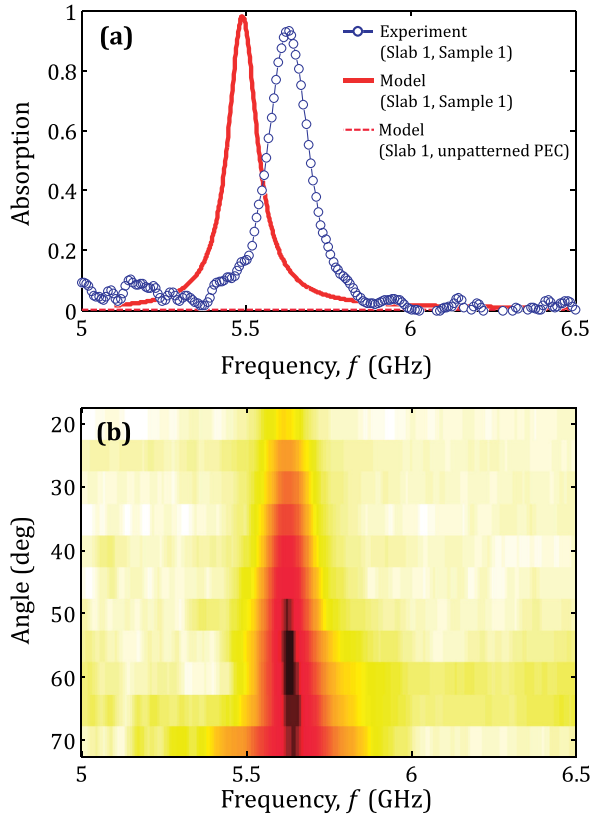

FIG. 2. (a) Absorption spectrum obtained with an incident p-wave with $\theta = 45°$. The structure is formed by a combination of sample 1 ($h = 10$ mm) with slab 1 ($\ell = 1.2$ mm) (see Fig. 1). (b) Experimental absorption spectra taken for several incidence angles θ, where the darkest color corresponds to the strongest absorption.

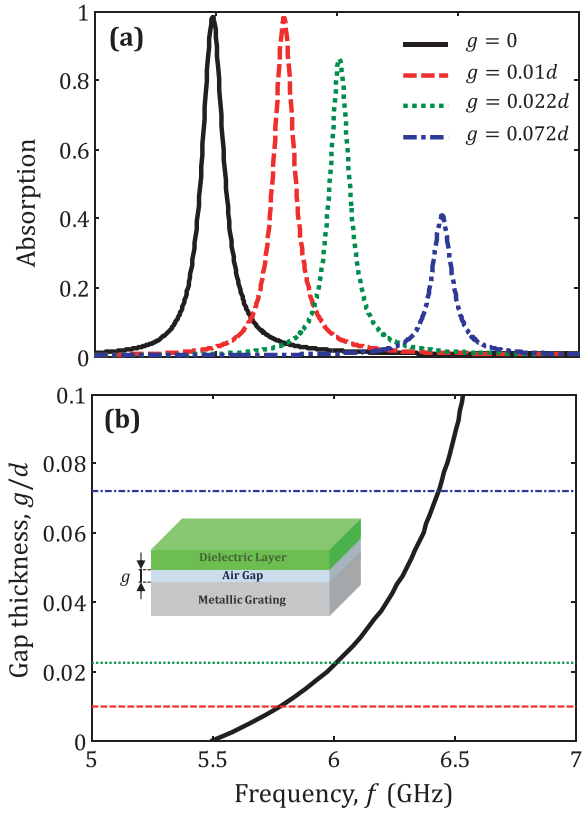

FIG. 3. Effect of non-perfect contact between the dielectric layer and the metallic grating on the frequency of the absorption peak (numerical predictions) for the sample 1 ($h = 10$ mm) with the slab 1 ($\ell = 1.2$ mm) when the incidence angle is $\theta = 45°$. (a) Calculated absorption spectra for several values of air gap thickness, g. (b) Calculated position of the absorption peak as a function of the air gap thickness, g. The inset illustrates the structure studied here.

produced during the manufacturing process of the coaxial cavities edges, and because of the mechanical stress of the dielectric layer, which is not completely flat. The effect of the non-perfect contact between the dielectric and the metasurface is discussed later. In Figure 2(b), the same type of measurement has been performed for several incident angles; from $\theta = 20°$ to $\theta = 70°$, respectively. The observed insensitivity of the peak position with the impinging angle supports the predictions of the model.[16] Nevertheless, the absorption amplitude changes, a maximum value is achieved for $\theta = 60°$ while for higher or lower angles the absorption decreases. Also, it is easy to observe that, when the incidence angle is close to normal incidence ($\theta \approx 0$), the absorption vanishes because the impinging wave cannot excite the resonant modes in the coaxial cavities without a phase variation across the surface.

To get a physical insight of the frequency shift observed between theory and experiment, we have extended the model introduced in Ref. 16 to the case that considers an air gap between the dielectric layer and the metal grating [see inset in Figure 3(b)]. The model is comprehensively described on Sec. 1 in the supplementary material.[18] A parametrical study of the air gap thickness, denoted by g, has been performed for $\theta = 45°$ using slab 1 on top of sample 1. Figure 3(a) represents the absorption spectra calculated for several values g showing how the existence of an air gap shifts the absorption peak to higher frequencies. This behavior supports our previous claim suggesting that an unavoidable air gap explains the discrepancy between theoretical results and experimental data observed in Fig. 2(a). Moreover, in Fig. 3(b), the frequency position of the peak is represented as a function of g. This curve is obtained using Eq. (S32) of the supplementary material.[18] In this figure, the horizontal lines correspond to air gap thicknesses of the spectra shown in Fig. 3(a). In our experimental setup, it is not possible in practice to ensure a perfect contact between the metal and the dielectric surfaces. The effect of the air gap has been studied in all the measurements presented in this work, and the results of these studies are reported in Table I. In what follows, the measured results are compared with results obtained using the model that takes into account the air gap correction.

Now, we experimentally study the feasibility of tuning the peak position with the cavity length, h. To do that, we have employed the dielectric layer with $\ell = 1.2$ mm (slab 1) and the three metallic surfaces (Sample 1, 2 and 3 in Table I). The corresponding spectra are shown in Fig. 4. The experimental data (symbols) are compared with the theoretical results (continuous lines) obtained with the semi-analytical model described in Sec. 1 of the supplementary material[18] (continuous lines). The measured (calculated) peaks appear at 5.62(5.62) GHz, 7.24(7.24) GHz, and 9.14(9.14)GHz for $h = 10$ mm, $h = 7$ mm and $h = 5$ mm, respectively. The calculated profiles are fitted using the following air gap

TABLE I. Effect of an air gap on the frequency of the peak showing total absorption. The g values are obtained from the fitting to the measured peak position.

System	Model without air gap ($g = 0$)	Model with an air gap (g)		Experiment
	f (GHz)	g (μm)	f (GHz)	f (GHz)
Sample 1 + slab 1	5.5	36	5.62	5.62
Sample 2 + slab 1	7.09	30	7.24	7.24
Sample 3 + slab 1	8.83	41	9.14	9.14
Sample 2 + slab 2	6.88	36	7.09	7.09
Sample 2 + slab 3	6.68	41	6.92	6.92

thicknesses: $g = 36\,\mu$m, $30\,\mu$m, and $41\,\mu$m, respectively. These results demonstrate the tuning capability of the absorption peak with h while keeping its high absorption (>90%). The measured (calculated) peak amplitudes are 0.93 (0.99), 0.99 (0.99), and 0.97 (0.99) for $h = 10$ mm, $h = 7$ mm, and $h = 5$ mm, respectively. From these results, one can conclude that it would be possible to introduce a methodology allowing the design of structures with total absorption at given frequencies. The reader is addressed to Sec. 2 in the supplementary material where such design methodology is comprehensively described with examples.[18]

The role that the dielectric layer thickness (ℓ) plays in determining the amplitude and frequency position of the total absorption peak produced by a given patterned surface is now analyzed. We have considered the metasurface sample 2 having patterned cavities with $h = 7$ mm and successively covered with the three dielectric slabs which are over the optimum value of ℓ. Figure 5 shows the three absorption spectra obtained for $\theta = 45°$, the symbols represent the measurements while the continuous lines illustrate the theoretical simulations. It is observed that changes of the layer thickness are accompanied with changes in the position and amplitude of the absorption peak. The measured (calculated) frequencies of the absorption peaks are 7.25(7.25) GHz, 7.09 (7.09)GHz, and 6.92 (6.92) GHz for $\ell = 1.2$ mm, $\ell = 1.6$ mm, and $\ell = 2.3$ mm, respectively. The calculated spectra are obtained using an air layer with $g = 30\,\mu$m, $36\,\mu$m, and $41\,\mu$m,

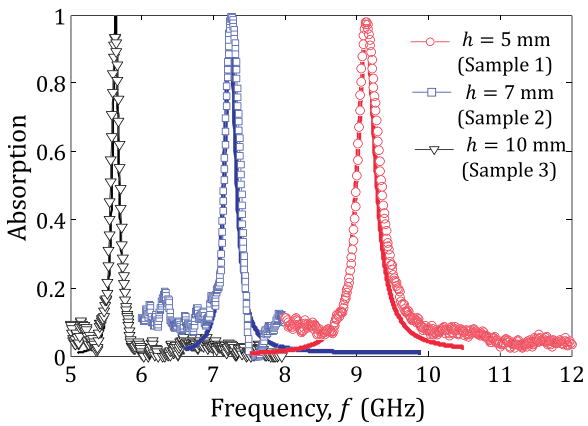

FIG. 4. Absorption spectra for three values of cavity length h. The dielectric thickness is $\ell = 1.2$ mm (slab 1) and the angle of incidence is $\theta = 45°$. Symbols represent the measurements and continuous lines represent the results obtained with the semi-analytical model.

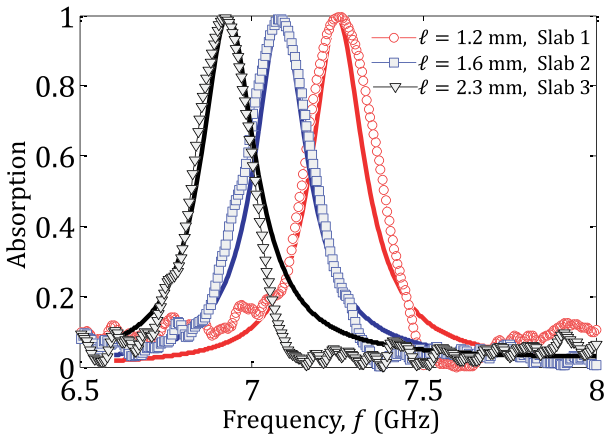

FIG. 5. Absorption for the sample 2 ($h = 7$ mm) with three different dielectric thicknesses. The angle of incidence is $\theta = 45°$. Symbols represent the measurements and solid lines represent the theoretical model.

respectively. The profiles show an almost perfect agreement with the experimental ones, except for the asymmetrical profile not shown in the numerical simulations. This asymmetry is probably due to an artifact of our experimental setup which uses finite size samples, a feature that is hard to include in our simulations. In other words, the receiver antenna is not symmetrically located with respect to the borders of the samples and, therefore, the waves radiated from the sample borders arrive to this antenna with low but different amplitudes, producing interference effects in the recorded spectra. This interference effects are clearly observed in the wiggling observed at the lower (absorption) parts of the spectra. The measured (calculated) peak amplitudes are 0.99(0.99), 0.98(0.99), and 0.99(0.99) for $\ell = 1.2$ mm, $\ell = 1.6$ mm, and $\ell = 2.3$ mm, respectively. A detailed study of the effect of the dielectric thickness is reported on Sec. 3 in the supplementary material[18] where it is shown that the optimum ℓ value for h = 7 mm is $\ell_{opt} = 0.8$ mm. For values $\ell > \ell_{opt}$, the low frequency absorption peak will exhibit total absorption.

In summary, this work has reported experimental evidence of total absorption for p-polarized waves impinging a thin absorbing layer deposited on top of coaxial-type cavities patterned on a metallic plate. The array of cavities has a subwavelength periodicity. The experimental data demonstrate how the resonances produced by the metallic grating enhance over 3300% the absorption in the low-loss dielectric layer, compared to the response with an unpatterned metal backing. The behavior for different incidence angles has been also studied, demonstrating our previous findings regarding the independence of the peak position and the amplitude variations. The control of the absorption peak positions with the cavity length has been also demonstrated, thus supporting the theoretical predictions. The effects observed by changing the thickness of the dielectric layer have shown that total absorption can be obtained even with ultra-thin layers. Finally, a semi-analytical model, which includes an air layer in between the dielectric layer and the metallic metasurface, has been developed. The model was successfully employed to get a physical insight of the experimental results.

This work was partially supported by the Spanish Ministerio de Economía y Competitividad (MINECO) under

Contract No. TEC2010-19751 and the USA office of Naval Research, under Grant No. N000141210216. A. Hibbins acknowledges support from the UK Grant No. EEBB-I-1408331. We thank useful discussions with Daniel Torrent and the technical help of Benjamin Tremain.

[1]N. Engheta and R. W. Ziolkowski, *Metamaterials: Physics and Engineering Explorations* (Wiley–IEEE Press, Piscataway, NJ, 2006).
[2]R. Marqués, F. Martín, and M. Sorolla, *Metamaterials with Negative Parameter: Theory, Design, and Microwave Applications* (Wiley–Interscience, Piscataway, NJ, 2008).
[3]J. B. Pendry, D. Schurig, and D. R. Smith, Science **312**(5781), 1780 (2006).
[4]W. Cai, D. A. Genov, and V. M. Shalaev, Phys. Rev. B **72**(19), 193101 (2005).
[5]N. I. Landy, S. Sajuyigbe, J. J. Mock, D. R. Smith, and W. J. Padilla, Phys. Rev. Lett. **100**, 207402 (2008).
[6]H. Tao, N. I. Landy, C. M. Bingham, X. Zhang, R. D. Averitt, and W. J. Padilla, Opt. Express **16**, 7181 (2008).
[7]Y. Cheng, Y. Nie, and R. Gong, Opt. Laser Technol. **48**, 415 (2013).
[8]A. Hibbins, J. Sambles, C. Lawrence, and J. Brown, Phys. Rev. Lett. **92**, 143904 (2004).
[9]J. S. White, G. Veronis, Z. Yu, E. S. Barnard, A. Chandran, S. Fan, and M. L. Brongersma, Opt. Lett. **34**, 686 (2009).
[10]E. K. Stone and E. Hendry, Phys. Rev. B **84**, 035418 (2011).
[11]E. Lansey, I. R. Hooper, J. N. Gollub, A. P. Hibbins, and D. T. Crouse, Opt. Express **20**, 24226 (2012).
[12]H. Xiong, J. Hong, C. Luo, and L. Zhong, J. Appl. Phys. **114**, 064109 (2013).
[13]Y. Avitzour, Y. A. Urzhumov, and G. Shvets, Phys. Rev. B **79**, 045131 (2009).
[14]Y. Cui, K. H. Fung, J. Xu, H. Ma, Y. Jin, S. He, and N. X. Fang, Nano Lett. **12**, 1443 (2012).
[15]F. Ding, Y. Cui, X. Ge, Y. Jin, and S. He, Appl. Phys. Lett. **100**, 103506 (2012).
[16]A. Díaz-Rubio, D. Torrent, J. Carbonell, and J. Sánchez-Dehesa, Phys. Rev. B **89**(24), 245123 (2014).
[17]E. L. Holzman, IEEE Trans. Microwave Theory Tech. **54**(7), 3127 (2006).
[18]See supplementary material at http://dx.doi.org/10.1063/1.4922801 for a detailed study of the air gap and the effect of the dielectric thickness.